Fault Detection and Isolation for Non-Linear Systems Using Autonomous Multiple Models

Olívia M. A. Coelho [*] **, Leonardo R. Rodrigues** [**]

[*] *Embraer S.A., São José dos Campos, SP, (e-mail: olivia.coelho@embraer.com.br)*
[**] *Instituto Tecnológico de Aeronáutica, São José dos Campos, SP, (e-mail: leonardolrr2@fab.mil.br)*

Abstract: Real-time fault detection and isolation capability has become a competitive differential for modern, complex systems due to the increasing demand for higher levels of both reliability and safety. The use of health monitoring algorithms can be considered a powerful decision tool and a key enabler for new maintenance and logistic strategies in which decisions are made based on the estimated health condition of the systems under consideration. This paper presents the study of a fault detection and isolation (FDI) algorithm for non-linear systems based on a multiple-model architecture. The Extended Kalman Filter (EKF) is used as residual generation tool while the Autonomous Multiple Models (AMM) algorithm is used for residual evaluation. Numerical experiments are conducted to assess the performance and the limitations of the algorithm. The study covers an assessment of the algorithm sensitivity to different failure intensities and also its response to failures not initially considered in the fault detection and isolation architecture.

Keywords: Fault Detection and Isolation; Non-Linear Systems; Health Monitoring; Multiple Models; Extended Kalman Filter.

1. INTRODUCTION

As systems continue to become more complex and automated, the demand for high levels of performance, reliability, and availability keeps pushing the advent of new health monitoring technologies and paradigm changes regarding maintenance and logistics strategies (Goebel *et al.*, 2017).

In a highly globalized and competitive world, performance standards rise every day and systems must deliver the expected performance with high reliability levels. Therefore, the ability to detect and predict failures using real-time embedded systems is a competitive differential that has drawn attention to the development of Prognostic and Health Monitoring (PHM) techniques in several industry sectors such as aeronautical (Verhulst *et al.*, 2022)(Pollock *et al.*, 2021), automotive (Choi and Lee, 2022), and nuclear power (Shi *et al.*, 2018). Monitored systems present increased safety and robustness, avoiding catastrophic consequences that may originate from an undetected faults. In addition, PHM technologies come as key enablers for concepts such as Condition-Based Maintenance (CBM) (Li *et al.*, 2020), Performance-Based Logistics (PBL), maintenance scheduling, and spare parts management (Rodrigues and Yoneyama, 2020).

In this context, Fault Detection and Isolation (FDI) is a key concept that consists in detecting that the monitored system is performing outside the defined tolerances (fault detection) and identifying, amongst a set of candidate failure modes, which one is the root cause of the erratic behavior (isolation) (Ding, 2008). The techniques applied to implement the FDI capability are commonly classified as model-based or data-driven approaches (Thirumarimurugan *et al.*, 2016). Model-based approaches use the knowledge of the plant (mathematical or empirical) to build a model and compare the system current state with the expected state based on the model to detect faults, whereas data-driven approaches rely on collected measurement data to identify healthy and faulty patterns.

A common approach used in FDI systems is to build a models bank containing models that represent the behavior of the monitored system in the presence of a set of failure modes of interest. A model that represents the healthy behavior of the system is also included in the bank. This FDI architecture isolates the failure mode by comparing the residuals between the system output and the output of each model belonging to the model bank. This approach is referred to as Multiple-Models Algorithms (MMA) (Magill, 1965).

The literature contains different generations of MMAs. The differences among these generations are associated with the type of interactions among the models belonging to the model bank. In this paper, a first generation MMA is used in a model-based FDI architecture applied to a non-linear system.

This paper aims at contributing to the literature on first generation MMA-based FDI methods by implementing and investigating the performance of a first generation MMA. Numerical experiments were conducted to assess the behavior of the algorithm considering the gradual evolution of failure modes. Also, the behavior of the algorithm

when the monitored system is subjected to a failure mode not included in the model bank is investigated.

The remaining sections of this paper are organized as follows. Section 2 describes the Model-Based Fault Detection concept. Section 3 presents a brief description of the Kalman Filter algorithm. Section 4 discusses the use a multiple model strategy for FDI purposes. Section 5 presents the different generations of multiple-model algorithms. Section 6 presents the case study considered in this paper to evaluate the performance of the proposed FDI strategy. Section 7 shows the results obtained in the numerical experiments. Concluding remarks are given in section 8.

2. MODEL-BASED FAULT DETECTION

The model-based fault detection concept is very intuitive. If a model that describes the monitored system is available, as well as the measurement of the system input and output, the model output can be computed and compared with the measured output. The difference between the measured output and the output computed with the model is called residual (Ding, 2008). Considering an ideal scenario in which there are no disturbances and the model is a perfect representation of the monitored system, the residual will be zero while the system is healthy. When the monitored system starts to behave differently from the expected, the residual will then become different from zero. Therefore, by monitoring the residual the faults can be detected.

Despite the simplicity of the model-based fault detection concept, the uncertainties observed in real applications make it a real engineering challenge. The model used to represent the monitored system may have limitations that are related to model complexity. The model fidelity may need to be compromised to guarantee a limited computational power, especially when dealing with real-time applications. In addition, the fault detection architecture will be subjected to disturbances such as process noise $w(t)$ and measurement noise $v(t)$, which will interfere in the relationship between the system input $u(t)$ and the observed output $z(t)$. Therefore, the residual generated will never be zero, even when the system is in its healthy state.

Besides the plant model, the residual-based FDI architecture contains a residual generator and a residual evaluator. In order to make the architecture more robust to the uncertainties, filters or estimators can be used as residual generators (Venkateswaran *et al.*, 2022). Additionally, to achieve successful and robust residual evaluation, statistical methods are commonly used (Zhou and Zhu, 2021).

3. RESIDUAL GENERATION USING KALMAN FILTER

A well-known technique used as a robust residual generator is the Kalman Filter (Kalman, 1960). The Kalman Filter is a predictor-corrector estimator which provides an optimal solution for linear dynamic systems corrupted with white noise. Therefore, its application as a residual generator uses the disturbance characteristics, which shall be Gaussian noise so that the Kalman Filter output minimizes the error covariance of the system state estimate.

On the FDI architecture, the plant model is replaced with a Kalman Filter built based on the plant model. The innovation sequence (differences between the filter prediction and the measured output) is used as residue, as shown in Figure 1. In order to determine the system health state, the innovation sequence properties are analyzed. If the system and model dynamics match, the innovation sequence will have the properties of white Gaussian noise.

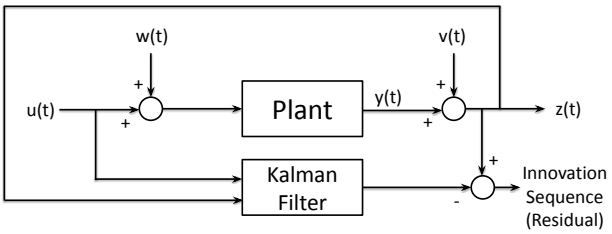

Figure 1. Model-based residual generation using a Kalman Filter.

The application of the classical Kalman Filter is restricted to linear dynamic systems which are subjected to Gaussian noise. Variations of the method and alternatives were developed to address these limitations such as the Extended Kalman Filter (EKF) (Jazwinski, 1970), the Unscented Kalman Filter (UKF) (Julier and Uhlmann, 1997), and the Particle Filter (PF) (Gordon *et al.*, 1993).

The EKF is a variation of the Kalman Filter based on the linearization of the model equations to be applied to non-linear systems. The EKF linearizes a non-linear state transition function $f_k(.)$ and a measurement function $g_k(.)$ around the mean of the current state estimate. At each time step, the linearization is performed locally using Taylor series expansion (Anderson and Moore, 1979). The EKF uses the same recursive process as the classical Kalman Filter, only with adaptations to project the state and error covariance ahead and to compute the Kalman gain.

4. FDI USING MULTIPLE MODELS

If only one model of the system representing its healthy behavior is used, it is possible to detect deviations of the plant behavior from the expected dynamics, but it is not possible to identify which failure mode is causing the degraded behavior. However, if a set of different models representing several possible system failure modes is used, the plant current condition can be isolated by evaluating the residual generated by each model, assuming that one of the models contemplates the plant current condition.

In order to build a multiple-model FDI architecture, a set of models is assembled containing a model for the healthy condition and one additional model for each faulty state that shall be monitored. The residuals generated by each model are computed simultaneously, and the model that generates the smallest residual is chosen as best candidate to represent the system current state.

Using Kalman Filters or EKFs as the residual generation tool, a filter bank can be built based on the models bank, and the innovation sequence that most resembles

a Gaussian noise will indicate the system state. Figure 2 shows the model-based FDI architecture using the EKF as a residual generation tool considered in this paper.

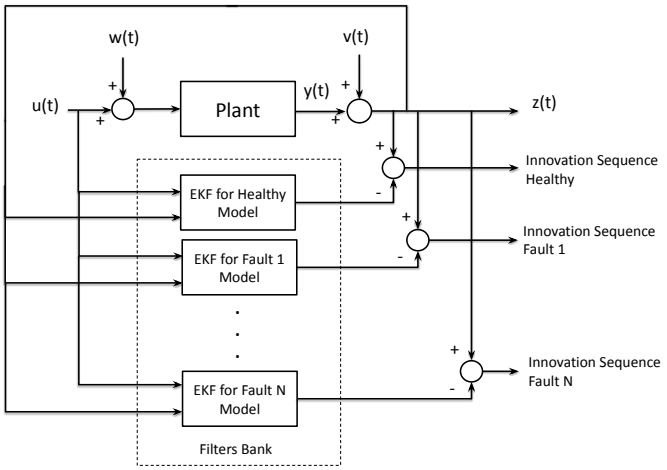

Figure 2. Model-based FDI architecture using EKF.

Each filter in the proposed architecture will result in an individual prediction time series to be evaluated. In order to combine the output of each filter in the filter bank into an overall estimate of the current system state, a Multiple Model Algorithm (MMA) strategy can be applied.

5. MULTIPLE-MODEL ALGORITHMS

The MMA consists of estimate-decision based algorithms comprising the following steps (Pitre, 2004):

(1) Build the model bank with the possible candidates for the system state;
(2) Run the set of filters, each based on a unique model;
(3) Combine the outputs of the filters into an overall likelihood estimate for the system state.

The overall estimate will present the likelihood that the system current state matches each candidate model. The fundamental assumption of the algorithms is that the true state of the system is represented in the model set. The multiple-model algorithms are classified into three generations (Bar-shalom and Blair, 2000), and there are studies for the application of all generations on FDI problems:

(1) **First Generation - Autonomous:** the models do not use information from other models in the bank (Coelho *et al.*, 2019);
(2) **Second Generation - Cooperative:** the filters interact with each other to provide a better estimate (Judalet *et al.*, 2015);
(3) **Third Generation - Variable Structure:** use a variable structure model set (Ru and Li, 2008).

The first generation algorithms were introduced by Magill (1965). Solutions that combine the outputs of elemental filters have been proposed for fault detection and fault-tolerant control applications with promising results (Coelho *et al.*, 2019), (Kargar *et al.*, 2014).

Motivated by the real-time target tracking problem for abruptly changing systems, a second generation MMA was developed by Blom (1984). This generation introduces interactions among the elemental filters. The overall estimate considers past information from all elemental filters to achieve better performance. The Interactive Multiple Model (IMM), a second generation MMA, is widely applied to target tracking applications (Vasuhi and Vaidehi, 2016) (Xie *et al.*, 2018), as well as for fault detection and isolation (Tudoroiu and Khorasani, 2005) (Zhang and Chen, 2019).

The first two MMA generations assume that one of the elemental filters in the bank represents the system true mode. However, there are situations in which this assumption does not hold. In order to address this limitation with reduced computational cost, the third generation MMA was introduced by Li (1994). These algorithms do not have a fixed model bank. Instead, their structure adapts over time. Therefore, unlike the fixed structure MMA, they use the measurement information not only to calculate the overall estimate but also to adjust the model set. Applications of variable structure MMA for fault detection and isolation have been proposed by Ru and Li (2008) and Lu *et al.* (2015).

In this paper, a first generation MMA referred to as Autonomous Multiple Model (AMM) is used. As a first generation MMA, the AMM algorithm has two fundamental assumptions (Li and Jilkov, 2005): (i) the true mode is time-invariant; and (ii) the true mode at any time is identical to one of the models in the model set. In order to compute the overall estimate, the filters run in parallel independently from one another. The algorithm fuses the individual output from the filters to calculate the probability that the true mode matches each one of the models in the model set.

The probability calculations are based on each model's likelihood. The model likelihood is updated in each time step using information up to the current time step as shown in Eq. (1).

$$L_k^{(i)} = p[z_k|m^{(i)}, z_{k-1}] = \mathcal{N}(\tilde{z}_k^{(i)}; 0; S_k^{(i)}) \tag{1}$$

where $L_k^{(i)}$ is the likelihood function of model $m^{(i)}$ given that $m^{(i)} \in \mathbb{M}$ (models set), $\mathcal{N}(x; \mu; \sigma^2)$ is the Gaussian probability density function of x with mean μ and standard deviation σ, $\tilde{z}_k^{(i)}$ is the residual or prediction error (innovation sequence). The mean μ is considered to be zero and the standard deviation is given by the measurement prediction error covariance $S_k^{(i)}$ of model (i) at instant k.

The model probability $\mu_k^{(i)}$ given by Eq. (2) is calculated based on the model likelihood and indicates the probability of model $m^{(i)}$ be the true mode at time k. Equation (2) is a weighted average using the models likelihood as the weights and normalized to guarantee that the sum of all probabilities will always be one.

$$\mu_k^{(i)} = \frac{\mu_{k-1}^{(i)} L_k^{(i)}}{\sum_{j \in \mathbb{M}} \mu_{k-1}^{(j)} L_k^{(j)}} \tag{2}$$

The selection of the MMA generation to be used in each application is a trade-off between performance and complexity. This paper brings an assessment of the EKF-AMM algorithm application and also aims at investigating the algorithm response when its main assumptions are not met, detailing a study of the algorithm sensitivity to different failure intensities and also its response to failures not initially considered in the model set.

6. CASE STUDY

A case study is presented to illustrate the application of the presented method. The model considered in this case study was built based on a laboratory bench presented in Jha *et al.* (2016). This laboratory bench consists of an electro-mechanical rotational system. The system comprises an electric motor, a pulley and belt set, motor and load disks, bearings, and a flexible shaft as illustrated in the block diagram presented in Figure 3.

The non-linearity in the system consists of a non-linear resistance representing the frictional torque over the motor disk. This frictional torque, denoted by τ_{Mech}, manifests due to Coulomb friction and is calculated by multiplying the frictional force f_{mech} by the radius of the motor disk r_{Md}, as defined in Eq. (3). The frictional force f_{mech} is defined in Eq. (4) in terms of the friction coefficient β, the suspended load mass M, the Earth's gravitational acceleration g, and the motor disk angular velocity ω_{Md} (Jha *et al.*, 2016).

$$\tau_{Mech} = f_{mech} \times r_{Md} \tag{3}$$

$$f_{Mech} = \beta M g \left(\frac{\omega_{Md}}{|\omega_{Md}|} \right) \tag{4}$$

The state transition model of the system is described in Equations (5) to (8).

$$x_1(k+1) = \Big(\begin{bmatrix} -\frac{R_a}{L_a} & -\frac{n_1}{J_m} & 0 & 0 \end{bmatrix} \boldsymbol{x_k} + u_k \Big) Ts + x_1(k) \tag{5}$$

$$\begin{aligned} x_2(k+1) = \Big(& \frac{n_1}{L_a} x_1(k) - \\ & \Big(f_m + n_2^2 \Big(J_{Ld} + b_{Md} + \beta M g r_{Md} \frac{x_3(k)}{|x_3(k)|} \Big) \frac{1}{J_{Md}} \Big) x_2(k) + \\ & \frac{-n_2}{C_s} x_3(k) \Big) Ts + x_2(k) \end{aligned} \tag{6}$$

$$x_3(k+1) = \Big(\begin{bmatrix} 0 & \frac{n_2}{J_m} & 0 & -\frac{1}{J_{Ld}} \end{bmatrix} \boldsymbol{x_k} \Big) Ts + x_3(k) \tag{7}$$

$$x_4(k+1) = \Big(\begin{bmatrix} 0 & 0 & \frac{1}{C_s} & -\frac{b_{Ld}}{J_{Ld}} \end{bmatrix} \boldsymbol{x_k} \Big) Ts + x_4(k) \tag{8}$$

Considering that there is a current sensor in the DC motor and an angular speed sensor in the load bearing, these two measured variables were defined as the system outputs. They correspond to states x_1 and x_3, respectively. The state-space equations were implemented in MATLAB®. Table 1 presents the values used for the parameters.

6.1 Failure Modelling

Three failure modes are considered throughout this paper. They are referred to as motor, bearing, and shaft failures. The selection of the failure modes took into account the separation of their effects on the system. There must be enough separation so that they can be individually identified.

(1) R_{deg1}: represents an electrical motor failure;
(2) R_{deg2}: represents an increased friction in the pulley bearing;
(3) C_{deg}: represents a change in the flexible shaft elasticity;

For the case study, R_{deg1} is considered as an increase of 65% in R_a; R_{deg2} as an increase of 150% in b_{Md}; and C_{deg} as a reduction of 50% in C_s. The severity of the degradation levels were defined based on observations of the system response in several simulations.

7. EVALUATION OF THE PROPOSED FDI ALGORITHM

As mentioned earlier, the proposed FDI method uses the EKF as a residual generation tool and the AMM algorithm as a residual evaluation tool. The method implementation comprises five steps, as illustrated in Figure 4. The algorithm is executed at each time step individually for each filter in the bank. The results are fused only in the last step when the model probabilities are computed.

For the first part of the study, the candidate modes considered were: healthy system, system with motor failure, system with bearing failure, and system with simultaneous motor and bearing failures. Therefore, one model was built for each candidate system mode to compose the model bank. An EKF was built for each model and the architecture presented in Figure 2 was assembled. With the algorithm presented in Figure 4, a single overall estimate of the system current state can be computed at each time step.

The architecture was implemented using MATLAB® and a sampling time of 0.5 milliseconds was used, which was defined based on the system dynamics and filters performance. The input signal used was a sinusoidal wave with amplitude 100V and period π. Additionally, the signal-to-noise ratio considered was 20dB for both the measurement and process noise. The results for the simulation considering the healthy system are shown in Figure 5. The algorithm converged very quickly (less than 0.01s) to indicate 100% probability of the true mode being the healthy system.

The simulation was then repeated with the system in each failure state considered in the model bank: motor failure, bearing failure, and simultaneous bearing and motor failure. For all simulations, the algorithm correctly converged to indicate the true system state. For the motor and bearing single failures the algorithm took longer to converge when compared with the healthy system and

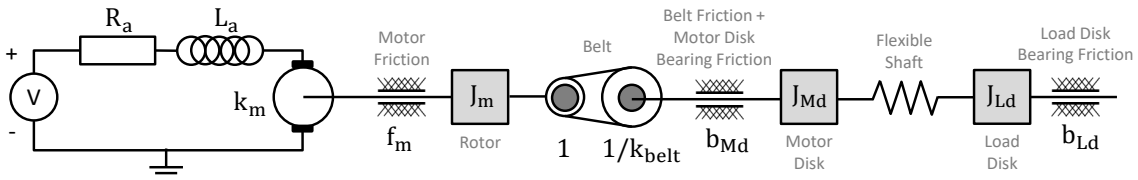

Figure 3. Case study system diagram (adapted from Jha *et al.* (2016)).

Table 1. Parameter Values

Symbol	Parameter	Value	Unit
R_a	Armature Resistance	1.23	Ω
L_a	Armature Inductance	1.34×10^{-3}	H
M	Suspended Load Mass	0.5	Kg
n_1 or k_m	DC Motor Torque Constant	2.57	A / (N · m)
n_2 or $1/k_{belt}$	Belt Constant	2.70	- - -
r_{Md}	Motor Disk Radius	0.1	m
β	Friction Coefficient on Motor Disk	0.8	- - -
J_{Md}	Motor Disk Moment of Inertia	9.00×10^{-2}	Kg · m^2 / rad
b_{Md}	Belt and Motor Disk Bearing Friction	4.22×10^{-1}	N · m · s / rad
C_s	Flexible Shaft Elasticity	1.79×10^{-1}	N · m / rad
J_{Ld}	Load Disk Moment of Inertia	6.70×10^{-3}	Kg · m^2 / rad
b_{Ld}	Load Disk Bearing Friction	5.10×10^{-1}	N · m · s / rad
f_m	Motor Friction	2.00×10^{-1}	N · m · s / rad
J_m	Rotor Moment of Inertia	6.76×10^{-3}	Kg · m^2 / rad

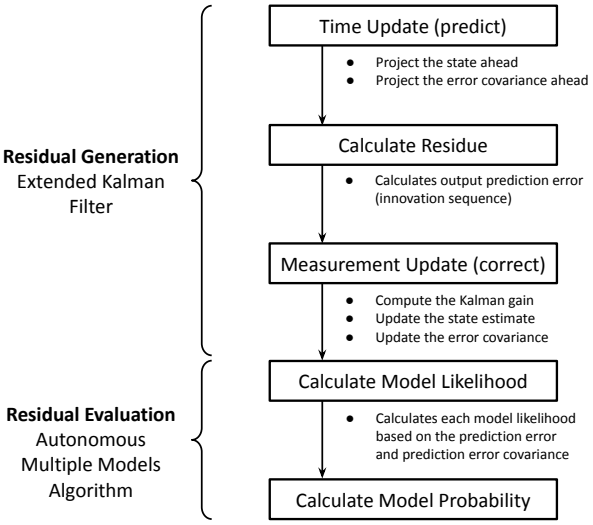

Figure 4. Steps to implement the proposed FDI algorithm.

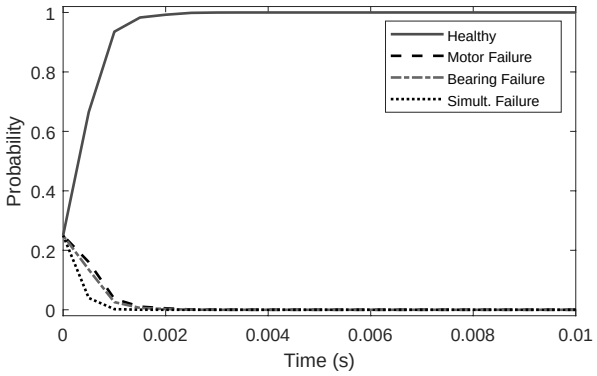

Figure 5. Simulation result for the healthy system.

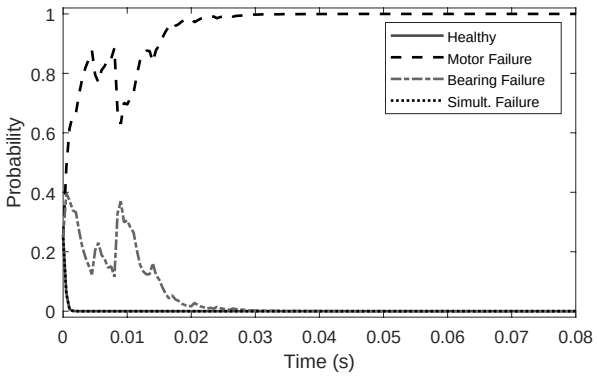

Figure 6. Motor failure simulation result.

simultaneous failure simulations. Figure 6 shows the result for a motor failure simulation.

In some simulations, it was observed that the algorithm initially converged to the wrong mode, but over time the estimate shifted to the correct state. Figure 7 illustrates an example of a bearing failure simulation where the algorithm initially indicated a motor failure. By analyzing the filters estimate for this simulation, it is possible to see in Figure 8 that for output y_1 the separation between the estimates is very subtle and for output y_2 the motor failure filter and bearing failure filter outputs are the closest ones.

Figure 8 shows another difference in the results when compared with the linear system implementation presented in Coelho *et al.* (2019). For the linear system, the Kalman Filter estimates for output y_1 showed more separation, contributing to a better system state identification. Nonetheless, the algorithm was able to correctly isolate the system state in all simulations with the non-linear system and EKF.

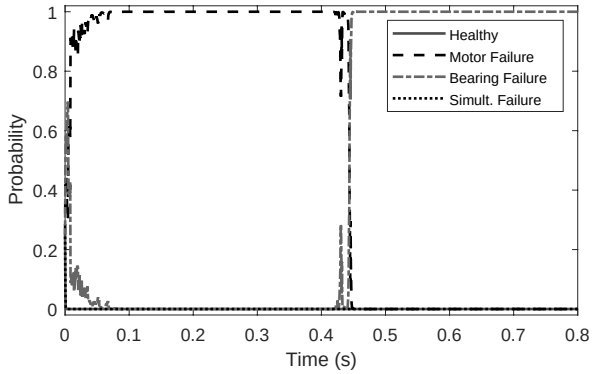

Figure 7. Simulation result in the presence of a bearing failure.

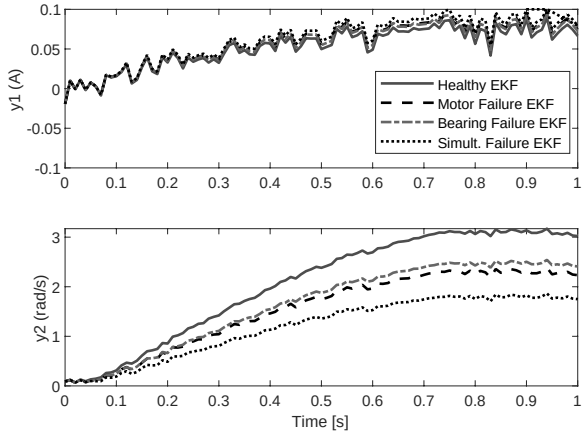

Figure 8. Filter estimate of a bearing failure simulation (Note: signal sampling time was reduced to aid visualization).

7.1 Algorithm Performance vs Failure Severity

The first set of simulations considered an ideal scenario in which the system state matched exactly one of the models in the model set. Even though this is one of the assumptions of the AMM, this assumption may not hold in real applications. Besides modeling approximations and errors, a failure mode in real systems may evolve gradually, with its severity increasing over time. For the motor and bearing failures, the failure mode evolution could be represented by a progressively change in the degradation value. In order to assess the algorithm sensitivity to failure severity, a set of simulations was conducted. For each simulation, it was checked how quickly the algorithm was capable of correctly identifying the failure. This time was defined as the instant when the correct model probability reached 90% and stayed above 90% until the end of the simulation.

For the motor failure simulations, the failure severity range used was from 0 up to an extra degradation of 100% of R_a, with a step of 1%. Figure 9 shows the result of the analysis. The x-axis represents the percentage of degradation in R_a and the y-axis shows the time that the algorithm took to correctly isolate the system state. A bold line marks the 0% degradation simulation (healthy system) and a dashed line marks the standard degradation (65% of R_a). The bars are plotted for each test case in which the failure was correctly isolated. For degradation levels lower than 40%, the algorithm was not able to detect the motor failure. Figure 10 brings the equivalent result for the bearing failure simulations. For degradation levels lower than 100% of b_{Md}, the algorithm was not able to detect the failure.

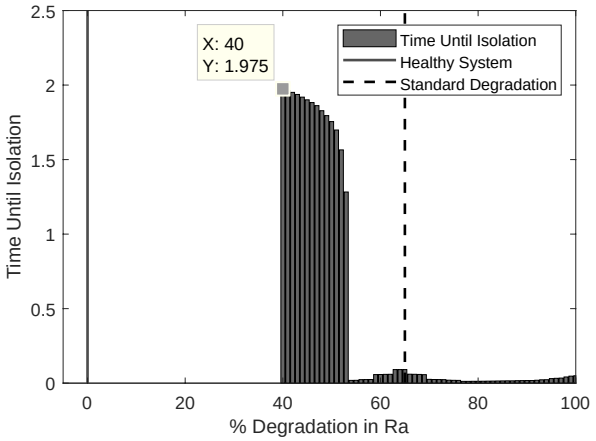

Figure 9. Time until isolation versus degradation severity for motor failure.

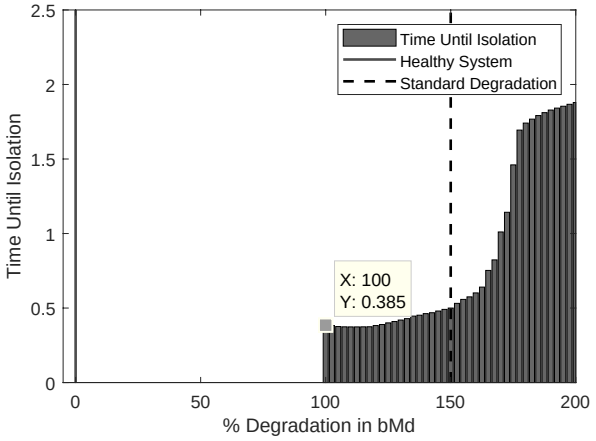

Figure 10. Time until isolation versus degradation severity for bearing failure.

The results presented herein for both failure modes correspond to a single set of simulations of a particular noise seed. The simulation was repeated for several noise seeds and the results obtained are slightly different for each run but the overall behavior remains the same. When comparing the results obtained with a similar analysis performed with the linear system implementation in Coelho *et al.* (2019), it can be observed that the threshold for the failure detection with the non-linear system was higher.

The algorithm was capable of correctly isolating both the motor and bearing failures in a considerable range of degradation levels, demonstrating robustness to variations on the failure severity and modeling errors. The range in which the failure was not identified is also important and is associated with the algorithm sensitivity. Algorithms with high sensitivity can often result in high false alarm rates

triggered by disturbances and uncertainties. In addition, small degradation levels may not affect the system overall performance and, therefore, do not require any immediate maintenance actions. On the other hand, safety-critical systems may require high sensitivity FDI methods depending on the hazard of the failure mode. Therefore, the application may require more sophisticated methods. The FDI algorithm sensitivity choice is highly dependent on the application.

7.2 Algorithm Response to a Failure not Modelled

Besides possible variations on the failure severity, another scenario that affects the AMM assumptions is when the system is subjected to a failure mode not considered in the model bank. The model considered in this case study has over 10 parameters and the motor and bearing failures consider changes in only two of them. All system parameters are prone to degradation, however, it may not be feasible to model all of the possibilities since this will directly affect the architecture complexity and, consequently, the computational effort required to run the algorithm.

In order to study the effects of a failure mode that was not considered in the model bank, a third failure mode referred to as shaft failure was considered. Using the architecture presented in Figure 2, the simulation was carried out with the system presenting a deviation of -50% in parameter C_s. In this simulation, the algorithm converged to isolate a simultaneous motor and bearing failure, indicating that the simultaneous failure EKF was the one that produced the lowest residual among all the models in the model bank.

When the FDI architecture was updated to include the shaft failure model in the model bank, the algorithm was capable of correctly isolating the failure mode. The result obtained with the updated model bank including the shaft failure model is shown in Figure 11.

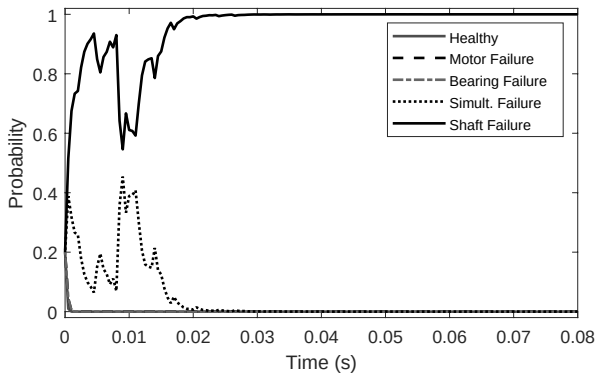

Figure 11. Flexible shaft failure simulation (failure included in model bank).

With this new failure mode, if desired to cover all multiple failure scenarios, four new models have to be added to the model bank. Therefore, in order to handle multiple failures with the proposed FDI architecture, a significant increase in the number of models is needed.

8. CONCLUSION

This paper presented the application of a model-based FDI algorithm based on EKF and multiple models to a case study of a generic electromechanical system. The simulations were performed using MATLAB®. The algorithm was capable of successfully detecting and isolating all failure modes considered in the model bank, which comprised single and dual failures. Due to the algorithm limitations and assumptions, the selection of the models to build the bank requires special attention to make sure that the relevant failure modes are captured and to avoid false positives.

Besides the performance of the algorithm under ideal conditions, the paper also presented an analysis of the impacts of degradation severity and failure modes not considered in the model bank on the performance of the algorithm. Both analyses provoke the algorithm assumption that one of the elemental filters represents the system true mode. The failure severity study also assessed the algorithm sensitivity. It was concluded that for the case study the algorithm demonstrated certain robustness to variations on the failure severity and modeling errors. Safety-critical systems that require high sensitivity FDI may require more sophisticated methods. For the analysis of the algorithm response to a failure not modeled, the failure was detected but incorrectly isolated, as expected. When the new failure mode was included on the model bank, the isolation was also successful. The addition of new failure modes can significantly increase the models bank size, especially if handling multiple failures.

The main motivation of this paper is the application of the studied model-based FDI for building powerful decision-making tools. Future work would include later generation multiple-model algorithms and implementation of alternative architectures for handling multiple failures.

ACKNOWLEDGEMENTS

The authors acknowledge the support of the Brazilian National Council for Scientific and Technological Development (CNPq) under Grant 423023/2018-7, and Embraer S/A.

REFERENCES

Anderson, B.D.O. and Moore, J.B. (1979). *Optimal Filtering*. Prentice-Hall, Inc., New Jersey.

Bar-shalom, Y. and Blair, W. (2000). *Multitarget-Multisensor Tracking*. Artech Print, Noorwood, MA.

Blom, H.A.P. (1984). An efficient filter for abruptly changing systems. In *IEEE Conference on Decision and Control*, 656–658.

Choi, C. and Lee, W. (2022). Fault diagnosis and tolerance on reliability of automotive motor control system: A review. *International Journal of Automotive Technology*, 23(4), 1163–1174.

Coelho, O.M.A., Vianna, W.O., and Yoneyama, T. (2019). Fault identification and isolation in dynamic systems using multiple models. In *Annual Conference of the PHM Society*, volume 11.

Ding, S.X. (2008). *Model-Based Fault Diagnosis Techniques*. Springer, Berlin, Heidelberg.

Goebel, K., Daigle, M., Abhinav, S., Sankararaman, S., Roychoudhury, I., and Celaya, J. (2017). *Prognostics: The Science of Making Predictions*. CreateSpace, NewYork, 1 edition.

Gordon, N.J., Salmond, D.J., and Smith, A.F. (1993). Novel approach to nonlinear/non-gaussian bayesian state estimation. In *IEE proceedings F (radar and signal processing)*, volume 140, 107–113. IET.

Jazwinski, A.H. (1970). *Stochastic Processes and Filtering Theory*. Elsevier, New York.

Jha, M.S., Dauphin-Tanguy, G., and Ould-Bouamama, B. (2016). Particle filter based hybrid prognostics for health monitoring of wncertain systems in bond graph framework. *Mechanical Systems and Signal Processing*, 75, 301–329.

Judalet, V., Glaser, S., Gruyer, D., and Mammar, S. (2015). Imm-based sensor fault detection and identification for a drive-by-wire vehicle. *IFAC-PapersOnLine*, 48(21), 1158–1164.

Julier, S.J. and Uhlmann, J.K. (1997). New extension of the kalman filter to nonlinear systems. In *Signal processing, sensor fusion, and target recognition VI*, volume 3068, 182–193. International Society for Optics and Photonics.

Kalman, R.E. (1960). A new approach to linear filtering and prediction problems. *Journal of basic Engineering*, 82, 35–45.

Kargar, S.M., Salahshoor, K., and Yazdanpanah, M.J. (2014). Multiple model-based fault detection and diagnosis for nonlinear model predictive fault-tolerant control. *Arabian Journal for Science and Engineering*, 39(10), 7433–7442. doi:10.1007/s13369-014-1252-y.

Li, X.R. and Jilkov, V.P. (2005). Survey of maneuvering target tracking. part v. multiple-model methods. *IEEE Transactions on Aerospace and Electronic Systems*, 41, 1255–1321.

Li, X. (1994). Multiple-model estimation with variable structure: some theoretical considerations. In *IEEE Conference on Decision and Control*, volume 2, 1199–1204.

Li, Y., Peng, S., Li, Y., and Jiang, W. (2020). A review of condition-based maintenance: Its prognostic and operational aspects. *Frontiers of Engineering Management*, 7, 323–334.

Lu, P., Van Eykeren, L., van Kampen, E.J., de Visser, C., and Chu, Q. (2015). Double-model adaptive fault detection and diagnosis applied to real flight data. *Control Engineering Practice*, 36, 39–57.

Magill, D. (1965). Optimal adaptive estimation of sampled stochastic processes. *IEEE Transactions on Automatic Control*, 10(4), 434–439.

Pitre, R. (2004). *A Comparison of Multiple-Model Target Tracking Algorithms*. Master's thesis, University of New Orleans, New Orleans.

Pollock, L., Abdelwahab, A.K., Murray, J., and Wild, G. (2021). The need for aerospace structural health monitoring: A review of aircraft fatigue accidents. *IJPHM and JAERO Joint Special Issue on PHM for Aerospace Systems*, 12(3).

Rodrigues, L.R. and Yoneyama, T. (2020). A spare parts inventory control model based on prognostics and health monitoring data under a fill rate constraint. *Computers & Industrial Engineering*, 148, 106724. doi:10.1016/j.cie.2020.106724.

Ru, J. and Li, X.R. (2008). Variable-structure multiple-model approach to fault detection, identification, and estimation. *IEEE Transactions on Control Systems Technology*, 16(5), 1029–1038.

Shi, L., Jia, H., Zhou, Z., Cheng, L., Yu, P., Huang, Y., and En, Y. (2018). Intelligent maintenance design of nuclear power system based on PHM. In *2018 Prognostics and System Health Management Conference (PHM-Chongqing)*, 797–801. doi:10.1109/PHM-Chongqing.2018.00142.

Thirumarimurugan, M., Bagyalakshmi, N., and Paarkavi, P. (2016). Comparison of fault detection and isolation methods: A review. In *2016 10th International Conference on Intelligent Systems and Control (ISCO)*, 1–6. IEEE International Conference on Intelligent Systems and Control, IEEE, Piscataway.

Tudoroiu, N. and Khorasani, K. (2005). Fault detection and diagnosis for satellite's attitude control system (acs) using an interactive multiple model (imm) approach. In *IEEE Conference on Control Applications*, 1287–1292.

Vasuhi, S. and Vaidehi, V. (2016). Target tracking using interactive multiple model for wireless sensor network. *Information Fusion*, 27, 41–53.

Venkateswaran, S., Liu, Q., Wilhite, B.A., and Kravaris, C. (2022). Design of linear residual generators for fault detection and isolation in nonlinear systems. *International Journal of Control*, 95(3), 804–820.

Verhulst, T., Judt, D., Lawson, C., Chung, Y., Al-Tayawe, O., and Ward, G. (2022). Review for state-of-the-art health monitoring technologies on airframe fuel pumps. *International Journal of Prognostics and Health Management*, 13(1).

Xie, G., Gao, H., Qian, L., Huang, B., Li, K., and Wang, J. (2018). Vehicle trajectory prediction by integrating physics- and maneuver-based approaches using interactive multiple models. *IEEE Transactions on Industrial Electronics*, 65(7), 5999–6008.

Zhang, Z. and Chen, J. (2019). Fault detection and diagnosis based on particle filters combined with interactive multiple-model estimation in dynamic process systems. *ISA Transactions*, 85, 247–261.

Zhou, J. and Zhu, Y. (2021). Identification based fault detection: Residual selection and optimal filter. *Journal of Process Control*, 105, 1–14.